Shrinkage movement analysis of reinforced concrete floors constructed in stages

A.K.H. Kwan[†] and P.L. Ng

Department of Civil Engineering The University of Hong Kong, Hong Kong, China

Abstract. Reinforced concrete floors constructed between movement restraints often crack seriously due to shrinkage after completion. One common mitigation measure is to construct the concrete floors in stages to allow part of the shrinkage movement to take place before completion. However, shrinkage movement analysis of concrete floors constructed in stages is quite cumbersome, as the structural configuration changes during construction, thus necessitating reanalysis of the partially completed structure at each stage. Herein, a finite element method for shrinkage movement analysis of concrete floors constructed in stages is developed. It analyses the whole structure, including the completed and uncompleted portions, at all stages. The same mesh is used all the time and therefore re-meshing and location matching are no longer necessary. This is achieved by giving negligibly small stiffness to the uncompleted portions, which in reality do not exist yet. In the analysis, the locked-in strains due to increase in elastic modulus as the concrete hardens and the creep of the hardened concrete are taken into account. Most important of all, this method would enable fully automatic shrinkage movement analysis for the purpose of construction control.

Keywords: concrete floor, construction control, creep, finite element, shrinkage.

1. Introduction

Shrinkage of concrete is the gradual reduction in dimension of the concrete with time. It may or may not induce tensile stresses large enough to cause cracking, depending on whether there are restraints against the shrinkage shortening movement of the concrete structure (Gilbert 1992, Nejadi and Gilbert 2004). If the concrete structure were connected to rigid supports restraining its shrinkage movement, significant tensile stresses could be induced and the concrete might eventually crack. If the concrete structure were connected only to flexible supports that are movable with minimum restraining action, no significant tensile stresses would be induced and the concrete would not crack due to shrinkage. In a concrete building, however, some of the supports have to be rigid in order to provide lateral stiffness. Thus, the floor areas between the rigid supports would have significant tensile stresses induced due to shrinkage. For this reason, shrinkage cracking is a common scene in concrete buildings. As shrinkage cracks are mostly through cracks, they have been causing water leakage, serviceability and durability problems.

Concrete structures are often constructed in stages. The construction sequence and schedule have great effects on the shrinkage movement of the structural elements. Consider a concrete floor supported at its two opposite ends by rigid shear walls and at its centre by a flexible column, as

---

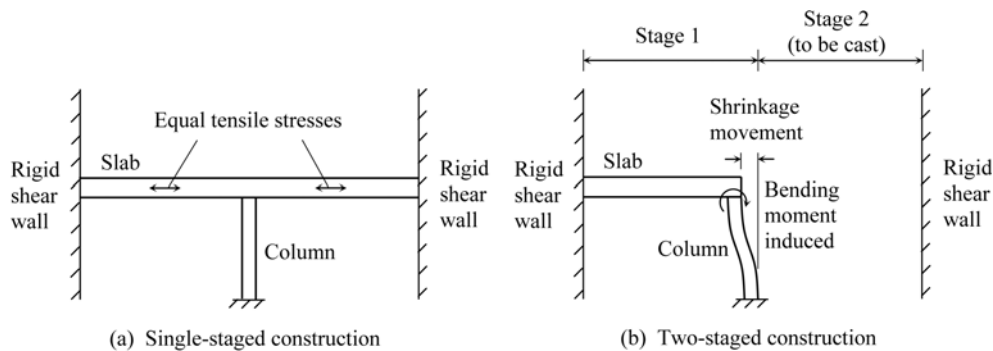† Professor, Corresponding author, E-mail: khkwan@hkucc.hku.hk

Fig. 1 Shrinkage of a floor restrained at two opposite ends

shown in Fig. 1(a). If the whole floor were cast in one concreting operation, then because of symmetry, there would be no shrinkage movement at the column head. However, as the floor shrinks, tensile stresses would be induced due to restraint of the shear walls against shrinkage movement. But, if the floor were constructed in two stages with half of the floor from the column to one shear wall cast first and the other half cast some time later, as depicted in Fig. 1(b), the column head would move during construction, thus causing the column to deform. Nevertheless, the two-stage construction would allow the portion cast in the first stage to shrink with little restraint before the remaining portion is cast, thus reducing the residual shrinkage when the floor is completed and the tensile stresses induced thereafter.

The analysis of movement and deformation during construction is within the scope of construction control, which aims to minimize the adverse effects or maximize the beneficial effects of such movement and deformation. For example, during the construction of cable-stayed bridges by launching the deck segments in stages, the time-dependent deck movement has to be analysed and monitored on site so that the cable forces can be adjusted to ensure perfect fitness upon closure of the deck segments (Han and Yan 2003). Construction control is also important in the construction of concrete buildings (Kwan *et al*. 2002). For a concrete building, the floors are usually constructed storey-by-storey. Even in the same storey, the floor could be cast in stages. During storey-by-storey construction, the differential shrinkage between the floors of adjacent storeys would cause deformation of the vertical elements and induce tensile stresses in the floors. During stage-by-stage construction of a floor in the same storey, the shrinkage of the partially completed floor would also cause deformation of the vertical elements but such relatively free shrinkage could reduce the residual shrinkage upon completion of the floor. This beneficial effect could be employed to minimize shrinkage cracking by providing a late-cast strip, which would not be cast until substantial shrinkage has taken place (Kwan *et al*. 2002, Kim and Cho 2004).

Shrinkage cracking is generally more serious in long concrete buildings (Kwan *et al*. 2002, Kim and Cho 2004, 2005). Depending on the shrinkage characteristics of the local concrete, the ultimate shrinkage strain could range from 400 to 800 $\mu\varepsilon$ (British Standards Institution, 1990, Comite Euro-International du Beton 1993). For a 100 m long concrete structure, the shrinkage shortening could amount to 100 m$\times$800 $\mu\varepsilon$ = 80 mm, and at each end, the shrinkage movement could be as large as 0.5$\times$80 mm = 40 mm. If there were rigid shear walls or even core walls near the ends, the shear/core walls would restrain the shrinkage movement (Kwan *et al*. 2003). In Hong Kong (the authors' home city), it is common to have a low-rise podium structure more than 100 m long with several

high-rise tower blocks on top but no movement joints provided. The shear/core walls supporting the tower blocks are constructed as integral parts of the podium structure and are so rigid that they hardly deflect at the podium level. Hence, the shrinkage movement of the podium structure is simply too large to be accommodated by the shear/core walls and, as a result, the podium structure would have to crack. In Hong Kong, even the high-rise buildings themselves can be as long as 60 m. Some of these buildings, which have shear/core walls located at their ends, are having the same cracking problem.

Because of the afore-mentioned cracking problem, the industry has been asking for shrinkage movement analysis software that can be used to assist the planning and design of construction control measures aimed at minimizing shrinkage cracking. For such shrinkage movement analysis, the finite element method, which can deal with complex two- and three-dimensional structures, should be the most suitable. However, shrinkage movement analysis is not at all easy. Firstly, as it takes months or even years for the shrinkage to finish, the tensile stresses induced would continue to develop for quite some time, during which creep would alleviate the tensile stresses. Hence, in any shrinkage movement analysis, the time-dependent shrinkage and creep effects should both be accounted for. Secondly, since the structural configuration changes during construction, the structure has to be re-analysed at each stage of construction as a different partially completed structure. Therefore, at each stage, the partially completed structure has to be re-meshed and the initial stress-strain condition of each finite element determined by location matching.

There have been only few studies on numerical shrinkage and creep analysis of concrete structures. Anderson (Anderson 1982) was among the earliest to apply the finite element method to such analysis. He divided the whole time period of interest into many time steps, performed finite element analysis at each time step to evaluate the time-dependent shrinkage and creep effects, and integrated the incremental strains and stresses with time to obtain the variations of the stress-strain conditions of the elements with time. Since then, such time step analysis and integration have become standard procedures (Jurkiewiez *et al*. 1999, Liu *et al*. 2006, Au *et al*. 2007). However, staged construction had not attracted much attention until the turn of the century. Recently, Kim and Cho (Kim and Cho 2004, 2005) have studied the shrinkage and creep in a multi-storey building constructed in stages by analysing a different partially completed structure at each stage of construction. Due to the change in structural configuration from stage to stage, the analysis was quite cumbersome.

Herein, a finite element method for shrinkage movement analysis of reinforced concrete floors constructed in stages is developed. Instead of analysing a different partially completed structure at each stage, the same structure, which comprises of both the completed and uncompleted portions forming the whole structure, is analysed at all stages, thus simplifying the data entry process, eliminating the necessity of re-meshing and location matching, and allowing fully automatic shrinkage movement analysis. The newly developed method has been validated by providing numerical examples to verify its accuracy and demonstrate its application to construction control.

2. Shrinkage and creep of concrete

2.1. Shrinkage

There are two main types of shrinkage, namely: autogenous shrinkage and drying shrinkage (Neville 1995). Autogenous shrinkage is caused by self-desiccation as water is being used up in the chemical reactions, without any movement of water into or out of the concrete. It has a variable magnitude but is in general fairly small compared to drying shrinkage and therefore in most practical applications, autogenous shrinkage is not distinguished from drying shrinkage. On the other hand, drying shrinkage is caused by loss of water from the concrete due to evaporation. As the loss of water with time depends on the permeability of the concrete, the size of the member and the conditions of the environment, the rate of drying shrinkage is dependent on these factors.

The shrinkage strain at any particular time is usually expressed as the product of the ultimate shrinkage strain and a dimensionless time function accounting for the variation of shrinkage with time. Let the ultimate shrinkage strain be ε_{cs0} and the time function be $\beta_s(t-t_s)$, in which t is the time being considered and t_s is the time when shrinkage starts. The shrinkage strain $\varepsilon_{cs}(t,t_s)$ at time t is given by

$$\varepsilon_{cs}(t,t_s) = \varepsilon_{cs0} \cdot \beta_s(t-t_s) \qquad (1)$$

Many different shrinkage models, giving different formulas for ε_{cs0} and $\beta_s(t-t_s)$, have been developed. In the proposed finite element method, any shrinkage model can be used. For illustration, the shrinkage model in Model Code 1990 (Comite Euro-International du Beton 1993) is adopted (in fact, the symbols used herein are largely the same as those in Model Code 1990). The ultimate shrinkage strain may be estimated using the formulas given in the shrinkage model or, if so demanded, directly measured using samples of the actual concrete in a laboratory. The time function is given in Model Code 1990 as

$$\beta_s(t-t_s) = \left[\frac{(t-t_s)}{\alpha_s + (t-t_s)} \right]^{0.5} \qquad (2)$$

where α_s is a coefficient governing the rate of shrinkage. The coefficient α_s is dependent on the thickness of the member and the temperature and relative humidity of the environment. It may be estimated using the formulas given in the shrinkage model or directly measured in a laboratory. From the time function, the shrinkage half-time $t_{0.5}$ (i.e. the time taken for half of the ultimate shrinkage strain to develop) may be obtained by solving the equation $\beta_s(t_{0.5}) = 0.5$ as $t_{0.5} = \alpha_s/3$.

2.2. Creep

The actual mechanism of creep is not yet thoroughly known (Neville 1995). Nevertheless, within the normal range of service stress, which is not expected to exceed 40% of the compressive strength of the concrete, the creep strain may be taken as proportional to the stress level (Neville 1995, Gilbert 1988). This proportionality forms the basis of the linear creep model, which has been incorporated in most codes of practice (British Standards Institution 1990, Comite Euro-International du Beton, 1993). In the proposed finite element method, any linear creep or other creep model (Ng *et al.* 2007) can be used, but for the sake of consistence, the linear creep model in Model Code 1990 (Comite Euro-International du Beton, 1993) is adopted.

In Model Code 1990, the elastic modulus at time t is denoted by $E_c(t)$. It is expressed as a fraction or multiple of the elastic modulus at the age of 28 days, $E_c(28)$, in the following form

$$E_c(t) = \beta_E(t) \cdot E_c(28) \tag{3}$$

where $\beta_E(t)$ is a function of the concrete age.

If a constant stress σ_c is applied at time t_0, the instant elastic strain $\varepsilon_{ce}(t,t_0)$ and the subsequent creep strain $\varepsilon_{cc}(t,t_0)$ are given respectively by

$$\varepsilon_{ce}(t,t_0) = \frac{1}{E_c(t_0)} \sigma_c(t_0) \tag{4}$$

$$\varepsilon_{cc}(t,t_0) = \frac{\phi(t,t_0)}{E_c(28)} \sigma_c(t_0) \tag{5}$$

in which $\phi(t,t_0)$ is the creep coefficient. Adding the elastic strain and the creep strain together, the total stress-dependent strain $\varepsilon_{c\sigma}(t,t_0)$ is obtained as

$$\varepsilon_{c\sigma}(t,t_0) = \frac{1}{E_c(t_0)} \sigma_c(t_0) + \frac{\phi(t,t_0)}{E_c(28)} \sigma_c(t_0) \tag{6}$$

The creep coefficient $\phi(t,t_0)$ above is given in Model Code 1990 in terms of

$$\phi(t,t_0) = \phi_0(t_0) \cdot \beta_c(t-t_0) \tag{7}$$

where $\phi_0(t_0)$ is the ultimate creep coefficient and $\beta_c(t-t_0)$ describes the development of creep with time. The coefficient $\phi_0(t_0)$ is dependent mainly on the concrete grade and the time at which the loading is applied whereas the function $\beta_c(t-t_0)$ is dependent mainly on the size of the member and the environmental conditions.

If the applied stress σ_c is not constant, the total stress-dependent strain may be evaluated using the principle of superposition (McHenry 1943, Ghali *et al.* 2002), which postulates that the response of concrete to a sum of two stress histories may be obtained as the sum of the individual response to each stress history. Based on this principle, the stress history is decomposed into a number of stress increments as in Fig. 2 and the elastic strain and creep strain caused by a variable stress $\sigma_c(\tau)$ are evaluated by summing the responses to the stress increments $\partial\sigma_c(\tau)$ each applied at time τ from t_0 to t as:
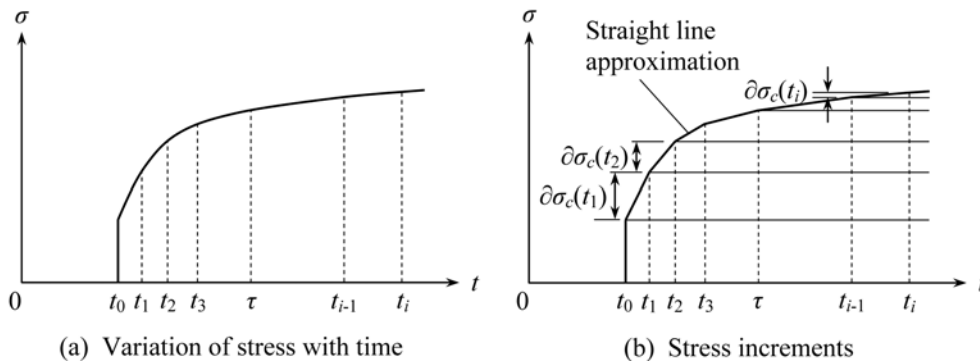

(a) Variation of stress with time   (b) Stress increments

Fig. 2 Decomposition of stress history into stress increments

$$\varepsilon_{ce}(t,t_0) = \frac{1}{E_c(t_0)}\sigma_c(t_0) + \int_{\tau=t_0}^{t} \frac{1}{E_c(\tau)}\partial\sigma_c(\tau) \tag{8}$$

$$\varepsilon_{cc}(t,t_0) = \frac{\phi(t,t_0)}{E_c(28)}\sigma_c(t_0) + \int_{\tau=t_0}^{t} \frac{\phi(t,\tau)}{E_c(28)}\partial\sigma_c(\tau) \tag{9}$$

From these, the total stress-dependent strain $\varepsilon_{c\sigma}(t,t_0)$ is obtained simply by adding the elastic strain $\varepsilon_{ce}(t,t_0)$ and the creep strain $\varepsilon_{cc}(t,t_0)$ together. In the actual finite element analysis, the stress history of each finite element is memorised and the above integrations are performed numerically using the trapezoidal rule.

3. Stress-strain relation of concrete

3.1. Incremental strain and stress

At any time t, the concrete strain $\varepsilon_c(t)$, which comprises of the shrinkage strain $\varepsilon_{cs}(t)$, creep strain $\varepsilon_{cc}(t)$, thermal strain $\varepsilon_{cT}(t)$ and elastic strain $\varepsilon_{ce}(t)$, is given by

$$\varepsilon_c(t) = \varepsilon_{cs}(t) + \varepsilon_{cc}(t) + \varepsilon_{cT}(t) + \varepsilon_{ce}(t) \tag{10}$$

Note that the shrinkage strain $\varepsilon_{cs}(t)$, creep strain $\varepsilon_{cc}(t)$ and elastic strain $\varepsilon_{ce}(t)$ are respectively the same as $\varepsilon_{cs}(t,t_s)$ in Eq. (1), $\varepsilon_{cc}(t,t_0)$ in Eq. (9) and $\varepsilon_{ce}(t,t_0)$ in Eq. (8). On the other hand, the thermal strain $\varepsilon_{cT}(t)$ may be evaluated simply by multiplying the temperature change up to time t with the coefficient of thermal expansion. The above equation may also be expressed as

$$\varepsilon_c(t) = \varepsilon_{cscT}(t) + \varepsilon_{ce}(t) \tag{11}$$

where $\varepsilon_{cscT}(t)$ denotes the sum of $\varepsilon_{cs}(t)$, $\varepsilon_{cc}(t)$ and $\varepsilon_{cT}(t)$.

Like other methods for the analysis of time-dependent effects, time step analysis is employed for the shrinkage movement analysis. Consider the $(i)^{th}$ time step. Let the beginning time and the ending time of the time step be t_{i-1} and t_i, respectively. The concrete strain $\varepsilon_c(t_{i-1})$ at time t_{i-1} and the concrete strain $\varepsilon_c(t_i)$ at time t_i are

$$\varepsilon_c(t_{i-1}) = \varepsilon_{cscT}(t_{i-1}) + \varepsilon_{ce}(t_{i-1}) \tag{12}$$

$$\varepsilon_c(t_i) = \varepsilon_{cscT}(t_i) + \varepsilon_{ce}(t_i) \tag{13}$$

Subtracting Eq. (13) by Eq. (12), we get

$$\Delta\varepsilon_c = \Delta\varepsilon_{cscT} + \Delta\varepsilon_{ce} \tag{14}$$

in which $\Delta\varepsilon_c$ is equal to $\varepsilon_c(t_i)$ minus $\varepsilon_c(t_{i-1})$, $\Delta\varepsilon_{cscT}$ is equal to $\varepsilon_{cscT}(t_i)$ minus $\varepsilon_{cscT}(t_{i-1})$ and $\Delta\varepsilon_{ce}$ is equal to $\varepsilon_{ce}(t_i)$ minus $\varepsilon_{ce}(t_{i-1})$.

Denoting the concrete stress at time t_{i-1} by $\sigma_c(t_{i-1})$ and the concrete stress at time t_i by $\sigma_c(t_i)$, the incremental concrete stress $\Delta\sigma_c$ may be expressed as $\sigma_c(t_i)$ minus $\sigma_c(t_{i-1})$. Based on Eq. (8), the incremental elastic strain $\Delta\varepsilon_{ce}$ in Eq. (14) may be expressed in terms of the incremental concrete stress $\Delta\sigma_c$ as

$$\Delta\varepsilon_{ce} = \frac{\Delta\sigma_c}{E_c(t_i)} \tag{15}$$

Substituting the above into Eq. (14) and rearranging, the incremental stress-strain relation of the concrete may be obtained as

$$\Delta\sigma_c = E_c(t_i)(\Delta\varepsilon_c - \Delta\varepsilon_{cscT}) \tag{16}$$

The above constitutive relation may be employed for incremental stress-strain analysis at the $(i)^{th}$ time step with the concrete strain $\varepsilon_c(t_{i-1})$ and concrete stress $\sigma_c(t_{i-1})$ at time t_{i-1} taken as the initial concrete strain and stress. Having evaluated the incremental concrete strain $\Delta\varepsilon_c$ and incremental concrete stress $\Delta\sigma_c$, the concrete strain $\varepsilon_c(t_i)$ and concrete stress $\sigma_c(t_i)$ at time t_i may be obtained as $\varepsilon_c(t_{i-1})$ plus $\Delta\varepsilon_c$ and $\sigma_c(t_{i-1})$ plus $\Delta\sigma_c$, respectively. After completing the analysis at the $(i)^{th}$ time step, such step-by-step incremental stress-strain analysis may be iterated until the shrinkage and creep of the concrete have largely finished.

3.2. Total strain and stress

Eq. (16) may also be expressed in terms of the total strains, $\varepsilon_c(t_{i-1})$ and $\varepsilon_c(t_i)$, and the total stresses, $\sigma_c(t_{i-1})$ and $\sigma_c(t_i)$, as:

$$\sigma_c(t_i) - \sigma_c(t_{i-1}) = E_c(t_i)((\varepsilon_c(t_i) - \varepsilon_{cscT}(t_i)) - (\varepsilon_c(t_{i-1}) - \varepsilon_{cscT}(t_{i-1}))) \tag{17}$$

Substituting Eq. (12) into the above equation, we get

$$\sigma_c(t_i) - \sigma_c(t_{i-1}) = E_c(t_i)(\varepsilon_c(t_i) - \varepsilon_{cscT}(t_i) - \varepsilon_{ce}(t_{i-1})) \tag{18}$$

Rearranging, the above equation becomes

$$\sigma_c(t_i) = E_c(t_i)(\varepsilon_c(t_i) - \varepsilon_{cscT}(t_i) - \varepsilon_{cl}(t_i)) \tag{19}$$

where $\varepsilon_{cl}(t_i)$ is given by

$$\varepsilon_{cl}(t_i) = \varepsilon_{ce}(t_{i-1}) - \frac{\sigma_c(t_{i-1})}{E_c(t_i)} \tag{20}$$

The term $\varepsilon_{cl}(t_i)$ is actually the locked-in strain due to gradual increase in elastic modulus of the hardening concrete. It has the physical meaning of the residual elastic strain when the stress is removed, as illustrated in Fig. 3. If there is no change in elastic modulus, the locked-in strain should remain the same.

Instead of incremental stress-strain analysis in terms of the incremental strain $\Delta\varepsilon_c$ and incremental stress $\Delta\sigma_c$, total stress-strain analysis in terms of the total strain $\varepsilon_c(t)$ and total stress $\sigma_c(t)$ may also be applied at each time step using the constitutive relation in Eq. (19). If total stress-strain analysis is applied, no initial strain and stress need to be considered; but the locked-in strain at each time step will have to be incorporated in the analysis.

Both the incremental stress-strain analysis and the total stress-strain analysis, which are mathematically equivalent to each other if all materials remain elastic, may be applied. They both have been attempted in this study and verified by examples presented hereafter to yield identical results under elastic condition. Nearly all existing methods are based on incremental stress-strain analysis (Anderson, 1982, Jurkiewiez *et al.* 1999, Kim and Cho 2004, 2005, Liu *et al.* 2006, Au *et*
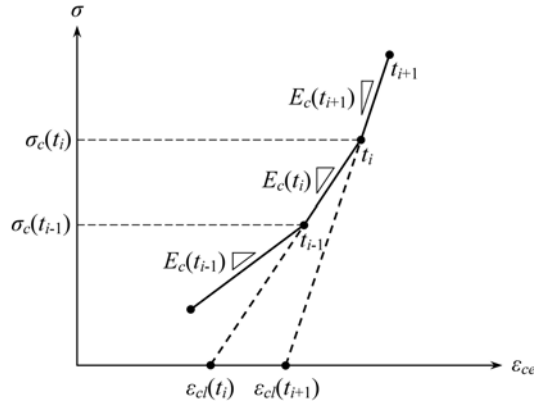
Fig. 3 Locked-in strain of hardening concrete under stress

al. 2007). However, the authors prefer total stress-strain analysis because total stress-strain analysis is more adaptable to future post-crack analysis, which is being explored and will be reported later. When concrete cracks, its tangent stiffness would become negative or even undefined and as a result any incremental stress-strain analysis would fail. With total stress-strain analysis, there should be no such problem.

4. Structural modelling and analysis

4.1. Finite element modelling

In the shrinkage movement analysis, all structural elements connected to the reinforced concrete floor are considered. There are two main types of structural elements, namely, horizontal elements and vertical elements. The horizontal elements are the slabs and beams constituting the floor whereas the vertical elements are the columns and shear/core walls supporting the floor. Although the horizontal and vertical elements together form a three-dimensional structure, only two-dimensional analysis of the in-plane behaviour of the floor is applied because the out-of-plane behaviour of the floor has little effect on the in-plane shrinkage movement. The structural elements are modelled by finite elements simulating their elastic, shrinkage, creep and thermal behaviour. Since the out-of-plane behaviour of the floor is not considered, each node has only two degrees of freedom, one being the horizontal displacement in one direction (along the x-axis) and the other being the horizontal displacement in the perpendicular direction (along the y-axis).

For the slabs, 3-noded triangular plane stress elements, with the steel reinforcing bars inside the concrete smeared to become continuously distributed, are used to model the reinforced concrete. Each plane stress element is actually composed of two elements superimposed onto each other, one modelling the concrete and the other modelling the smeared steel reinforcement. Taking into account the biaxial effects, the constitutive matrix equation of the concrete is derived from Eq. (19) as

$$\{\sigma_c\}_i = [D_c]_i(\{\varepsilon_c\}_i - \{\varepsilon_{cscT}\}_i - \{\varepsilon_{cl}\}_i) \qquad (21)$$

in which $[D_c]_i$ is the constitutive matrix of the concrete at time t_i, $\{\sigma_c\}_i$ is the stress vector of the concrete at time t_i, and $\{\varepsilon_c\}_i$, $\{\varepsilon_{cscT}\}_i$ and $\{\varepsilon_{cl}\}_i$ are the strain vector, shrinkage plus creep plus thermal strain vector and locked-in strain vector of the concrete at time t_i. The locked-in strain vector is derived from Eq. (20) as

$$\{\varepsilon_{cl}\}_i = \{\varepsilon_{ce}\}_{i-1} - [D_c]_i^{-1}\{\sigma_c\}_{i-1} \tag{22}$$

where $\{\varepsilon_{ce}\}_{i-1}$ and $\{\sigma_c\}_{i-1}$ are the elastic strain vector and stress vector of the concrete at time t_{i-1}. On the other hand, the constitutive matrix equation of the steel reinforcement is given by:

$$\{\sigma_s\}_i = [D_s]_i(\{\varepsilon_s\}_i - \{\varepsilon_{sl}\}_i) \tag{23}$$

in which $[D_s]_i$ is the constitutive matrix of the steel, and $\{\sigma_s\}_i$, $\{\varepsilon_s\}_i$ and $\{\varepsilon_{sl}\}_i$ are the stress vector, strain vector and locked-in strain vector of the steel at time t_i. Perfect bond between steel and concrete is assumed and thus the strain vector of the concrete $\{\varepsilon_c\}_i$ and the strain vector of the steel $\{\varepsilon_s\}_i$ are set to be equal.

For the beams, 2-noded bar elements, within which the steel reinforcing bars are superimposed onto the concrete, are employed. Derivations of the constitutive matrix equations of the concrete and steel in the bar element are similar to the above.

For the columns, each column is connected to one node on the floor at the centre of the column. The lateral stiffness of each column is modelled by two horizontal springs, one in each principal direction, as depicted in Fig. 4(a). In each principal direction, the column is assumed to deflect laterally in a contraflexural mode with the point of contraflexure located at mid-height of the column. With shear deformation incorporated, the lateral stiffness in each principal direction is given by

$$k_{cal} = \frac{1}{\dfrac{H^3}{12EI_c} + \dfrac{H}{\mu_c GA_c}} \tag{24}$$
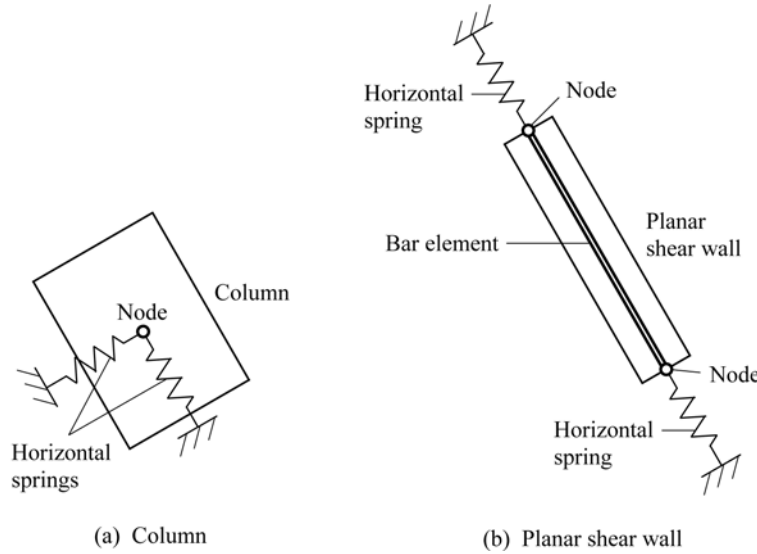

(a) Column   (b) Planar shear wall

Fig. 4 Modelling columns and planar shear walls

where H is the storey height, E and G are the elastic and shear moduli, and I_c, μ_c and A_c are the second moment of area, shape factor and section area of the column.

For planar shear walls, each wall is connected to two nodes on the floor, one at each end of the wall, as illustrated in Fig. 4(b). A bar element, with its width and depth taken to be the wall thickness and the storey height respectively, is added between the two nodes to model the in-plane elastic, shrinkage, creep and thermal behaviour of the wall. Two horizontal springs, both in the in-plane direction and one at each node, are added to model the in-plane lateral stiffness of the wall. In the in-plane direction, the wall is assumed to deflect laterally in a contraflexural mode with the point of contraflexure located at mid-height. With shear deformation incorporated, the in-plane lateral stiffness is given by

$$k_{wall} = \cfrac{1}{\cfrac{H^3}{12EI_w} + \cfrac{H}{\mu_w GA_w}} \tag{25}$$

where I_w, μ_w and A_w are the second moment of area, shape factor and section area of the wall. The above in-plane lateral stiffness is apportioned half to each of the two horizontal springs. Being rather small compared to the in-plane lateral stiffness, the out-of-plane lateral stiffness of the wall is neglected.

For nonplanar shear/core walls, each is considered as an assembly of planar wall units interconnected together. Nodes are placed at the ends of the wall units so that each wall unit is connected to two nodes, as shown in Fig. 5. For each wall unit, a bar element with its width and depth taken to be the wall thickness and the storey height respectively is added between its two end nodes to model the in-plane elastic, shrinkage, creep and thermal behaviour of the wall unit. To evaluate the lateral stiffness, each wall unit is considered in turn. Two horizontal springs, both in the in-plane direction and one at each end node, are added to model the in-plane lateral stiffness of the wall unit. As for the case of a planar shear wall, the out-of-plane lateral stiffness is neglected. The wall unit being considered is treated as a web while the other wall units connected to either end of the web are treated as flanges. The flange width of each flange is determined by cutting the flange

(a) Bar elements and horizontal springs   (b) Wall unit treated as an I-section
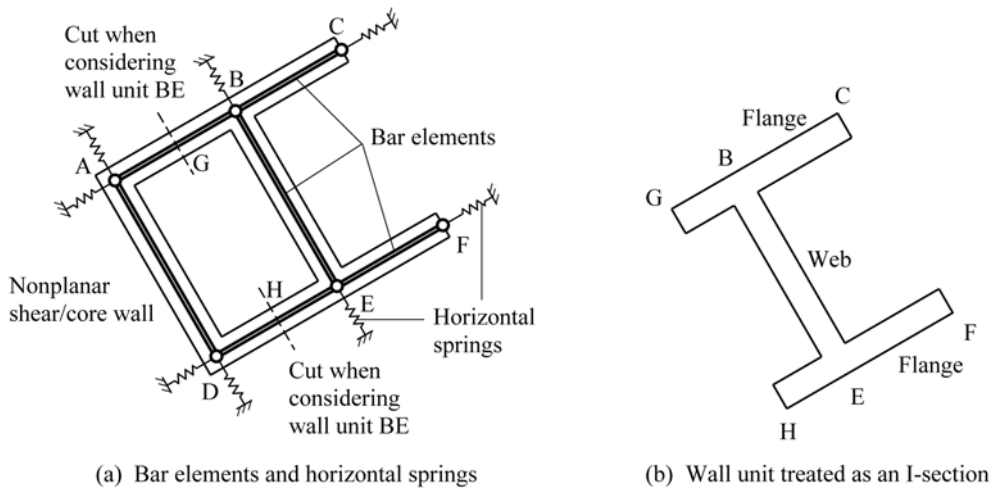
Fig. 5 Modelling nonplanar shear/core walls

at every mid-point between adjacent wall junctions. With the flanges appended, the wall unit becomes an I-section. The in-plane lateral stiffness of the wall unit is then evaluated using Eq. (25) with the section area A_w taken to be that of the web only. The in-plane lateral stiffness k_{wall} so evaluated is apportioned half to each of the two horizontal springs at the ends of the web. This procedure is repeated until every wall unit has been treated as a web to have its in-plane lateral stiffness modelled by a pair of horizontal springs.

4.2. Staged construction

Despite stage-by-stage construction, the whole floor, including the completed and uncompleted portions, is analysed at all times. The domain of the whole floor is divided into sub-domains, each corresponding to the portion to be constructed at a certain stage. During the mesh generation process, the finite elements are each assigned a label denoting the stage at which it will be constructed. Before starting the analysis, the time of casting and duration of curing of every stage of construction are entered so as to pass on such information through the label to the finite elements.

During the analysis, the finite elements within the uncompleted portions are given negligibly small stiffness and zero shrinkage, creep and thermal strains. Although in theory, the small stiffness of each uncompleted portion should be infinitesimally small, to avoid numerical difficulties, it is set equal to 10^{-5} times the corresponding stiffness when the portion is fully completed. As a result, even though the uncompleted portions do not exist yet, they can have finite strains induced and negligibly small stresses developed. No special numerical procedure is needed to deal with such finite strains before construction. When the incremental stress-strain analysis is applied, the finite strains before construction would automatically become the initial strains in the analysis because the strains obtained in the previous time step are always taken as the initials strains in the current time step. When the total stress-strain analysis is applied, the finite strains before construction would automatically become the locked-in strains when the concrete is cast, as can be seen from Eq. (20).

4.3. Demarcation of time steps

The time step analysis is performed from the time of casting of the first stage till the residual shrinkage strains of all the concrete have become insignificant. Depending mainly on the rate of shrinkage of the concrete, the total time period to be analysed could amount to 3 years or even longer. For accurate analysis, the total time period has to be divided into a number of small time steps. The authors have tried the use of a constant time step and found that in the practical cases analysed, the constant time step should not be longer than 2 days or otherwise the errors would be unacceptably large. However, with a constant time step of only 2 days, more than 500 time steps might be required and the computer time could become exceedingly long.

Generally, the rates of change of the elastic modulus, shrinkage strain and creep strain would all decrease with time. Setting a constant time step would lead to relatively large errors at the beginning and smaller errors at later time. To improve the overall accuracy and computational efficiency, it is proposed to use shorter time steps at the beginning and gradually lengthen the time steps as the analysis proceeds. One way of doing so is to set the time steps in the form of a geometric progression. Let the first time step be a, the second time step be ar, the third time step be ar^2 and so on, in which r is the common ratio. The elapsed time Δt after n such time steps is given by

$$\Delta t = a + ar + ar^2 + \ldots + ar^{n-1} = a\left(\frac{r^n - 1}{r - 1}\right)$$ (26)

Before the actual time steps could be demarcated, the times of the key events have to be determined first. The key events are casting of concrete, end of curing (or beginning of shrinkage) and reaching shrinkage half-time of each stage of construction. The time interval between two consecutive key events of the same stage is set as the elapsed time Δt. Many different combinations of a, r and n are possible for the given elapsed time. It is suggested that (1) the first time step a should be not longer than 1 day, (2) the number of time steps n from casting of concrete to end of curing should be at least 5, (3) the number of time steps n from beginning of shrinkage to reaching shrinkage half-time should be at least 50, and (4) the value of r should be within 1.05 to 1.15. Any set of a, r and n values satisfying these requirements may be adopted.

In the actual analysis, a geometric progression would start at casting of concrete and end at beginning of shrinkage and then a new geometric progression would start and continue at the same ratio r to beyond the shrinkage half-time. If any time step in a geometric progression is interrupted by a new stage of construction, the time step is shortened to suit and another geometric progression would start. Hence, over the entire period of analysis, the time steps form several geometric progressions with occasional deviations at the ends of the geometric progressions.

5. Examples

5.1. Floor structure studied

A podium structure with two core walls inside is taken as a typical example for the study. Fig. 6(a) shows the structural plan of the podium, which has an overall size of 90.0 m by 42.0 m and a storey height of 5.5 m. The floor slabs are 200 mm thick and provided with 0.4% reinforcement in both the x- and y-directions. The beams have uniform sections of 400 mm width by 600 mm depth and are provided with 1.0% reinforcement in the longitudinal direction. All the columns are square with a sectional size of 600 mm by 600 mm. Lastly, all the wall units forming the core walls have a thickness of 500 mm and are provided with 0.5% reinforcement in the horizontal direction. Fig. 6(b) shows the finite element mesh generated for the analysis.

The slabs and beams are cast of Grade 30 concrete with a mean 28-day cylinder strength of 37.0 MPa whereas the columns and core walls are cast of Grade 40 concrete with a mean 28-day cylinder strength of 48.0 MPa. Using Model Code 1990 (Comite Euro-International du Beton, 1993), the 28-day elastic modulus and tensile strength of Grade 30 concrete may be evaluated as 33.55 GPa and 2.9 MPa, respectively, while the 28-day elastic modulus and tensile strength of Grade 40 concrete may be evaluated as 36.27 GPa and 3.5 MPa, respectively. The Poisson's ratio of the concrete is taken as 0.18. On the other hand, the elastic modulus of the reinforcing steel is taken as 200 GPa.

In addition to the usual scheme of constructing the whole floor in one concreting operation (named as Scheme A), two alternative schemes of stage-by-stage construction (named as Scheme B and Scheme C) are also analysed to study the feasibility of applying construction control measures to reduce the shrinkage-induced tensile stresses. In Scheme B, the floor is constructed in two stages with half of the floor constructed in the first stage and the other half constructed 90 days later in the
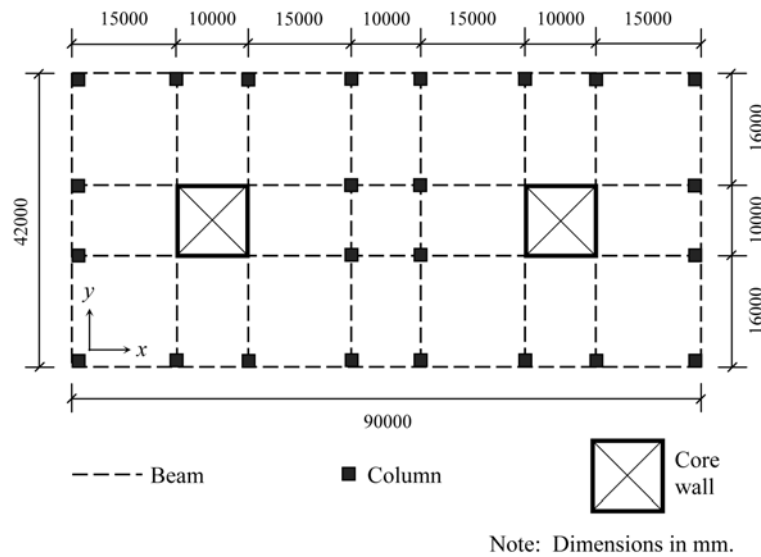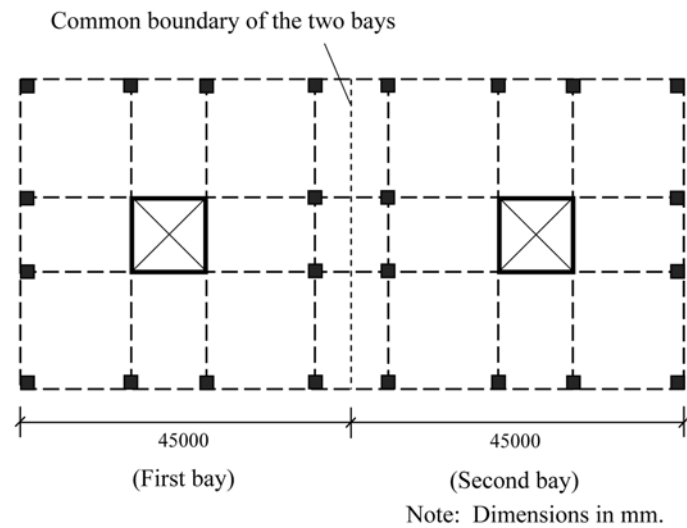
(a) Structural plan
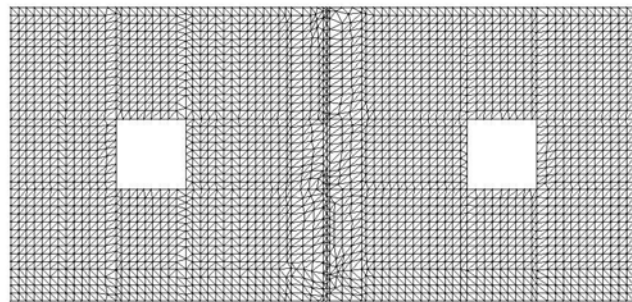
(b) Finite element mesh
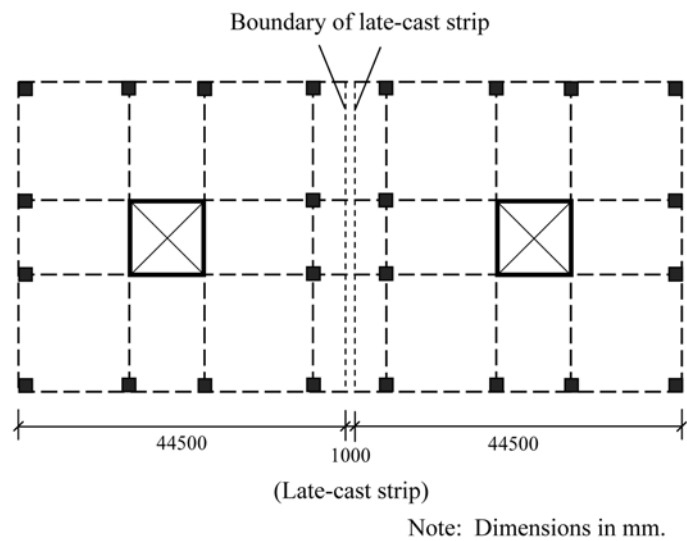
Fig. 6 Podium structure studied

second stage, as depicted in Fig. 7(a). In Scheme C, a late-cast strip is provided and the floor is also constructed in two stages. Basically the whole floor with the exception of a narrow strip (the late-cast strip) is constructed in the first stage and the late-cast strip is cast 180 days later in the second stage, as depicted in Fig. 7(b).

In the analysis, the environmental conditions are assumed to be uniform and constant at a temperature of 27°C and a relative humidity of 75%. For the evaluation of the shrinkage and creep strains, the shrinkage and creep models given in Model Code 1990 (Comite Euro-International du Beton, 1993) are adopted. In all the three schemes, the columns and core walls are assumed to be constructed 7 days ahead of the floor and the curing periods for all concrete members are assumed to be 5 days. The number of time steps adopted for the 5 days interval from casting of concrete to end of curing is 5 and the number of time steps adopted for the 307 days interval from beginning of shrinkage to shrinkage half-time of the 200 mm thick slabs is 50.

Two computer programs, one based on incremental stress-strain analysis and the other based on total stress-strain analysis, have been developed. Both have been applied to the following examples

Common boundary of the two bays

45000
(First bay)

45000
(Second bay)

Note: Dimensions in mm.

(a) Scheme B

Boundary of late-cast strip

44500

1000

44500

(Late-cast strip)

Note: Dimensions in mm.

(b) Scheme C

Fig. 7 Construction control schemes

and found to yield nearly identical numerical results with the absolute difference in induced strain generally less than 1%. Hence, only the numerical results obtained by the total stress-strain analysis are presented herein. Moreover, two different approaches, one with the uncompleted portions treated as non-existing and only the completed portions analysed as in the conventional methods and the other with both the completed and uncompleted portions incorporated in the analysis by giving a negligibly small stiffness to the uncompleted portions as proposed herein, have been attempted and found to yield basically the same numerical results with the absolute difference in induced strain generally less than 2%. The numerical results presented in the following are the results obtained by the proposed approach of incorporating both the completed and uncompleted portions in the analysis.
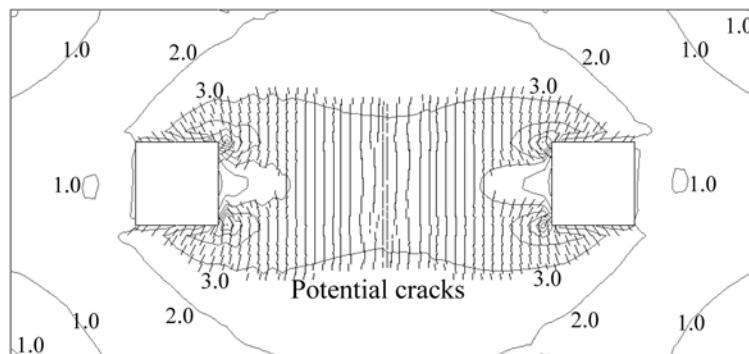
5.2. Scheme A: single-bay construction

In this scheme, the whole floor is cast in one concreting operation as a single bay, i.e., no construction control measure is applied to reduce the shrinkage-induced stresses. The resulting principal tensile stresses developed at 1 year and 3 years after casting of the floor are plotted in the form of stress contours in Fig. 8. At locations where the principal tensile stresses are greater than the tensile strength of the concrete, short straight lines indicating the potential crack directions are also drawn to indicate the potential crack areas and directions. From the figure, it can be seen that the slabs would start to crack within 1 year after casting. The extent of cracking would increase with time and at 3 years after casting, the cracking problem would become very serious. After 3 years, as most of the shrinkage should have taken place and the further increase in stress due to residual shrinkage would be largely compensated by the decrease in stress due to creep, there would be very little change in the shrinkage-induced stresses. Hence, the stress conditions at 3 years after casting may be taken to have reflected the long-term shrinkage and creep effects.
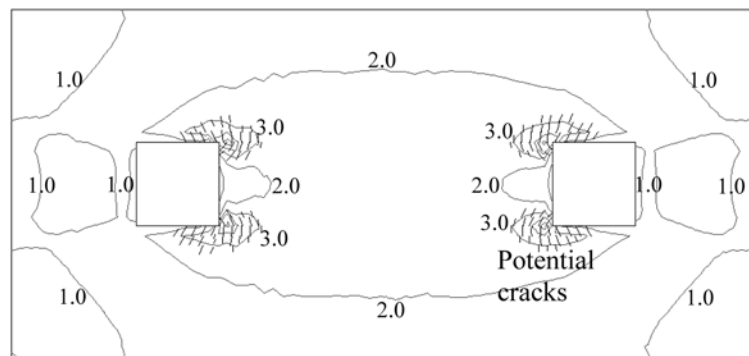
Note: Stresses in MPa.

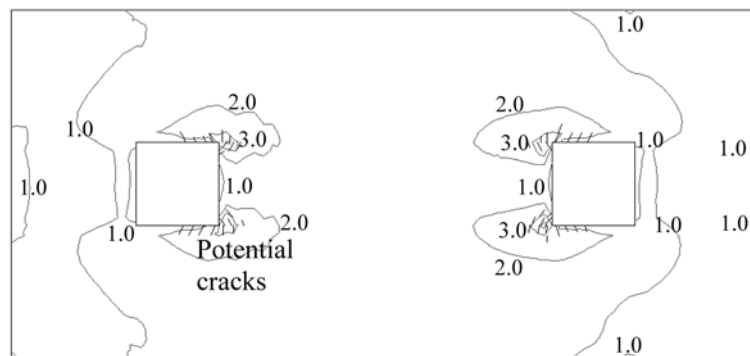(a) Principal tensile stresses and potential cracks after 1 year

Note: Stresses in MPa.

(b) Principal tensile stresses and potential cracks after 3 years

Fig. 8 Scheme A: single-bay construction

5.3. Scheme B: two-bay construction

In this scheme, half of the floor (the first bay) is cast first so that it can shrink without major movement restraint and the other half (the second bay) is cast 90 days later when part of the long-term shrinkage of the first bay has taken place, as in Fig. 7(a). To study the effectiveness of such construction control measure, the principal tensile stresses developed and the extents of cracking at 1 year and 3 years after the start of construction are plotted in Fig. 9 in the same way as before. Comparing with Fig. 8 for Scheme A, it can be seen that the shrinkage-induced stresses and the extents of cracking in Scheme B are noticeably smaller. Hence, with two-bay construction, the shrinkage cracking problem could be alleviated to a certain degree, although the slabs would still start to crack within 1 year after casting of the first bay. It is noteworthy that although the first bay is free to shrink for up to 90 days, after casting of the second bay, the shrinkage of the second bay would pull the first bay and induce tensile stresses therein, thus causing the first bay to crack also. After 3 years, the further increase in the shrinkage-induced stresses would be insignificant.

Note: Stresses in MPa.

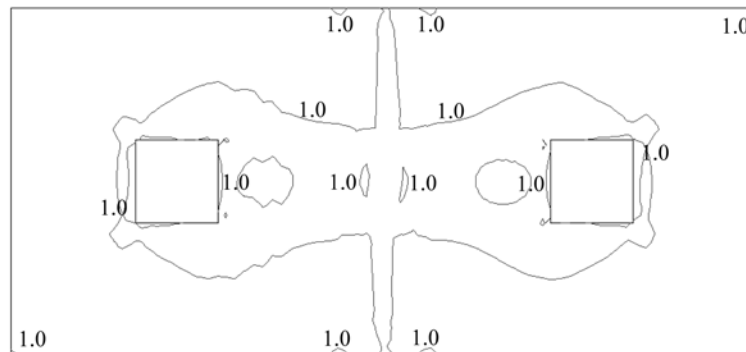(a) Principal tensile stresses and potential cracks after 1 year
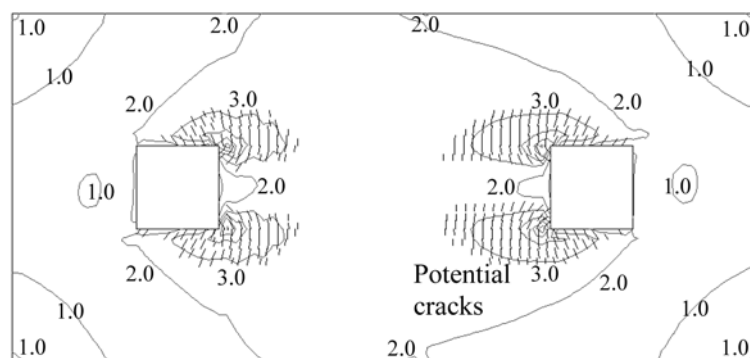
Note: Stresses in MPa.

(b) Principal tensile stresses and potential cracks after 3 years
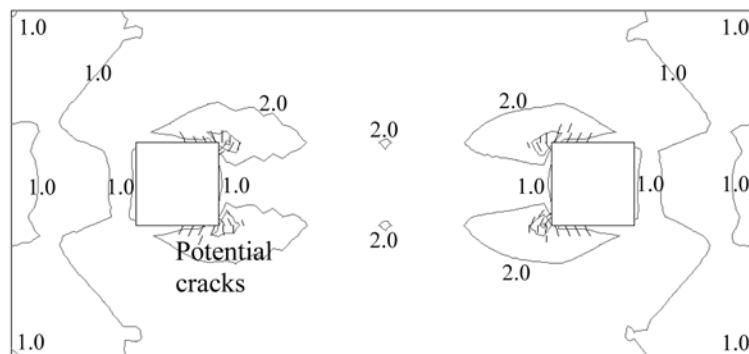
Fig. 9 Scheme B: two-bay construction

Note: Stresses in MPa.

(a) Principal tensile stresses and potential cracks after 1 year

Note: Stresses in MPa.

(b) Principal tensile stresses and potential cracks after 3 years

Fig. 10 Scheme C: provision of late-cast strip

5.4. Scheme C: provision of late-cast strip

In this scheme, in which a 1.0 m wide late-cast strip is provided, the whole floor with the exception of the late-cast strip is cast first and the late-cast strip is cast 180 days later when a substantial portion of the long-term shrinkage of the floor has taken place, as in Fig. 7(b). Before being closed, the gap at the late-cast strip acts as a temporary movement joint so that the floor areas already cast can shrink freely. To study the effectiveness of such construction control measure, the principal tensile stresses developed and the extents of cracking at 1 year and 3 years after the start of construction are plotted in Fig. 10 in the same way as before. Comparing with Fig. 8 for Scheme A and Fig. 9 for Scheme B, it can be seen that the shrinkage-induced stresses and the extents of cracking in Scheme C are the smallest. Hence, relatively, the provision of a late-cast strip should be a better construction control measure for alleviating the shrinkage cracking problem. As in the other schemes, after 3 years, there would be little further increase in the shrinkage-induced stresses. Anyway, due in part to the shrinkage of the late-cast strip itself, the shrinkage cracking problem has not been totally resolved. Other more effective construction control measures, e.g. the addition of an expanding agent into the late-cast strip (Neville 1995), should also be considered.

6. Conclusions

To analyse the extent of shrinkage cracking in a reinforced concrete floor or to evaluate the effectiveness of a construction control measure in alleviating shrinkage cracking, shrinkage movement analysis of the stage-by-stage constructed floor structure is needed. However, this is not at all easy because the structural configuration is changing during construction. In this paper, a new finite element method for the shrinkage movement analysis of reinforced concrete floors constructed in stages has been developed. Unlike the existing method of analysing a different partially completed structure at each stage of construction, the newly developed method analyses the whole structure, including the completed and uncompleted portions, at all stages by giving each uncompleted portion a negligibly small stiffness. With this method, there is no longer any necessity to re-mesh the partially completed structure and transfer the initial stress-strain conditions to the new mesh by location matching when the structural configuration changes. As a result, the same finite element mesh can be used for the analysis throughout. Data entry is needed only at the beginning of the analysis and no user intervention is required. In fact, the computer programs so produced by the authors based on this method are fully automatic.

Two alternative analytical procedures, an existing one based on incremental stress-strain analysis and a new one based on total stress-strain analysis, have been presented with all the basic equations derived for easy reference. The two analytical procedures are mathematically equivalent under elastic condition and have been verified to yield identical results in the examples given. However, the new total stress-strain analysis is preferred because when the shrinkage movement analysis is extended to the post-crack stage (such extension is highly recommended for further research so that the post-crack behaviour and the crack width could be evaluated), the existing incremental stress-strain analysis would encounter the major difficulty of negative or even undefined tangent stiffness. It is the authors' view that the best way of overcoming this major difficulty is to change to total stress-strain analysis.

The newly developed method has been applied to the construction control of the shrinkage cracking of a podium floor. It is shown that both bay-by-bay casting and provision of late-cast strips are effective in reducing the shrinkage-induced tensile stresses. Relatively, the provision of late-cast strips, which can be cast at a much later time when a substantial portion of the long-term shrinkage has taken place, is more effective. As demonstrated in the examples given, even when different construction control measures are applied, the same finite element mesh can be used. Hence, when testing different construction control measures for designing a suitable casting schedule, there is no need to regenerate the finite element mesh and only the areas to be cast, the time of casting and the period of curing in each stage need to be re-defined for analysis. This would make the tough job of construction control a lot easier.

References

Anderson, C.A. (1982), "Numerical creep analysis of structures", Creep and Shrinkage in Concrete Structures, edited by Bazant, Z.P. and Wittmann, F.H., John Wiley and Sons, New York, USA, 259-303.

Au, F.T.K., Liu, C.H. and Lee, P.K.K. (2007), "Shrinkage analysis of reinforced concrete floors using shrinkage-adjusted elasticity modulus", *Comp. Concrete*, **4**(6), 437-456.

British Standards Institution, BS5400: Part 4 Code of Practice for Design of Concrete Bridges, British Standards

Institution, UK, 1990.

Comite Euro-International du Beton, CEB-FIP Model Code 1990: Model Code for Concrete Structures, Thomas Telford Services Ltd., London, UK, 1993.

Ghali, A., Favre, R. and Elbadry, M. (2002), Concrete Structures: Stresses and Deformation, Third Edition, Spon Press, London, UK, 584.

Gilbert, R.I. (1988), Time Effects in Concrete Structures, Elsevier Science Publishers B.V., Amsterdam, The Netherlands, 321.

Gilbert, R.I. (1992), "Shrinkage cracking in fully restrained concrete members", ACI *Struct. J.* **89**(2), 141-149.

Han, D.J. and Yan, Q.S. (2003), "Cable force adjustment and construction control", Chapter 7, Bridge Engineering: Construction and Maintenance, Edited by Chen, W.F. and Duan, L., CRC Press, USA, 22.

Jurkiewiez, B., Destrebecq, J.F. and Vergne, A. (1999), "Incremental analysis of time-dependent effects in composite structures", *Comp. Struct.,* **73**(1-5), 425-435.

Kim, H.S. and Cho, S.H. (2004), "Shrinkage stress analysis of concrete slabs with shrinkage strips in a multistory building", *Comp. Struct.,* **82**(15-16), 1143-1152.

Kim, H.S. and Cho, S.H. (2005), "Shrinkage stress analysis of concrete slab in multistorey building considering variation of restraint and stress relaxation due to creep", *Struct. Des. Tall Special Build.,* **14**(1), 47-58.

Kwan, A.K.H., Au, F.T.K. and Lee, P.K.K. (2002), "Minimizing shrinkage cracks in concrete structures for better serviceability and durability", *Proceedings, Innovative Buildings Symposium, Hong Kong*, 117-136.

Kwan, A.K.H., Au, F.T.K. and Lee, P.K.K. (2003), "High-performance concrete buildings for the new millennium", *Prog. Struct. Eng. Mater.,* **5**(4), 263-273.

Liu, C.H., Au, F.T.K. and Lee, P.K.K. (2006), "Estimation of shrinkage effects on reinforced concrete podiums", HKIE *Transactions*, **13**(4), 33-43.

McHenry, D. (1943), "A new aspect of creep in concrete and its application to design", ASTM Proceedings, **43**, 1069-1084.

Nejadi, S. and Gilbert, I. (2004), "Shrinkage cracking and crack control in restrained reinforced concrete members", ACI *Struct. J.,* **101**(6), 840-845.

Neville, A.M. (1995), Properties of Concrete, Fourth Edition, Addison Wesley Longman Ltd., London, UK, 844.

Ng, P.L., Lam, J.Y.K. and Kwan, A.K.H. (2007), "Multi-layer visco-elastic creep model for time-dependent analysis of concrete structures", Proceedings, Eleventh International Conference on Civil, Structural and Environmental Engineering Computing, St. Julians, Malta, Edited by Topping, B.H.V., 17. (published in CD-ROM).